



# Optimization of process variables to prepare activated carbon from Noug (*Guizotia abyssinica* cass.) stalk using response surface methodology

Getasew Yirdaw<sup>a,\*</sup>, Awrajaw Dessie<sup>b</sup>, Tsegaye Adane Birhan<sup>b</sup>

<sup>a</sup> Department of Environmental Health Science, College of Medicine and Health Sciences, Debre Markos University, P.O Box 269, Debre Markos, Ethiopia

<sup>b</sup> Department of Environmental and Occupational Health and Safety, College of Medicine and Health Sciences, University of Gondar, P.O Box 196, Gondar, Ethiopia

## ARTICLE INFO

### Keywords:

Noug stalk  
Activated carbon  
Response surface methodology  
Surface area  
Yield

## ABSTRACT

Even though adsorption is considered the simple, effective, and efficient method for the treatment of wastewater, accessibility of low-cost and locally available activated carbon remains the challenge. In response to this, recently significant amounts of agricultural byproducts have been investigated to prepare low-cost porous carbon, but there is still a problem related to cost and availability. So, Noug stalk, chosen because of its abundance and low cost as an agricultural byproduct in Ethiopia, was chemically activated with phosphoric acid to produce a low-cost porous carbon. The production of Noug stalk activated carbon (NSAC) is optimized using response surface methodology. A central composite design was used to investigate the effect of three process parameters, namely carbonization temperature (450–650 °C), activation time (90–150 min), and impregnation ratio (w/w) (1–3), on the BET surface area and yield of porous carbon. The analysis of variance (ANOVA) result shows that all three process parameters showed a significant effect on the surface area of porous carbon, while only carbonization temperature showed a significant effect on the yield of porous carbon. The best conditions for NSAC preparation were a carbonization temperature of 537.50 °C, an activation time of 127 min, and an impregnation ratio of 1.95, resulting in a BET surface area and yield of 473.45 m<sup>2</sup> g<sup>-1</sup> and 53.78%, respectively. The expected and observed values of the model for the outcome variable were highly comparable. Several analytical techniques, including proximal analysis, Fourier transform infrared spectroscopy, and N<sub>2</sub> adsorption-desorption, were used to characterize the NSAC. The results demonstrated that the prepared NSAC has a highly porous structure comparable to porous carbon obtained from other biomass feedstocks. This implies it would be used as a potential low-cost alternative for wastewater treatment using the adsorption process.

**Abbreviations:** AC, Activated Carbon; ANOVA, Analysis of Variance; BET, Brunner-Emmett-Teller; CCD, Central Composite Design; FAAS, Flame atomic absorption spectrometry; FTIR, Fourier Transform Infrared Spectroscopy; NSAC, Noug Stalk Activated Carbon; RSM, Response Surface Methodology.

\* Corresponding author.

E-mail address: [gech23man@gmail.com](mailto:gech23man@gmail.com) (G. Yirdaw).

<https://doi.org/10.1016/j.heliyon.2023.e17254>

Received 9 December 2022; Received in revised form 10 June 2023; Accepted 12 June 2023

Available online 14 June 2023

2405-8440/© 2023 The Authors. Published by Elsevier Ltd. This is an open access article under the CC BY-NC-ND license (<http://creativecommons.org/licenses/by-nc-nd/4.0/>).

## 1. Introduction

Activated carbon is a well-known adsorbent that is utilized in a range of industries to remove, separate, retrieve and recover organic and inorganic molecules from gaseous and liquid streams [1]. Furthermore, activated carbon is commonly utilized to prevent pollution [2] and its harmful impacts on the environment [3]. Internal porosity, as well as related variables such as surface area, pore volume, pore size distribution, and the presence of functional groups on pore surfaces, all have a significant impact on porous carbon's capabilities [4,5]. The texture and other features of porous carbon are influenced by several conditions such as the type of the precursor material, the method of activation, the activating agent, and the type of activation process employed [5]. Porous carbon has been produced nowadays from a wide range of readily available and low-cost materials, such as agro-based products like teff straw [6], maize stalk & tassel [7,8], rice straw [9], and sunflower stalk [10].

The activated carbon can be prepared using two main procedures are used: physical activation and chemical activation. When compared to physical activation, chemical activation has two key advantages. First, chemical activation is accomplished at lower temperatures, whereas physical activation requires higher temperatures. Besides, chemical activation yields are higher since no burn-off char is required. Various chemicals, such as  $ZnCl_2$ ,  $H_3PO_4$ ,  $K_2CO_3$ ,  $KOH$ ,  $CaCl_2$ ,  $Na_2SO_4$ , and  $H_2SO_4$ , are employed in chemical activation [3]. The effect of chemical species on the characteristics of porous carbon has been widely investigated [11–13]. Phosphoric acid ( $H_3PO_4$ ) is a popular chemical reagent in the chemical activation method of synthesis of porous carbon because it improves pore formation in the porous carbon structure and results in a high carbon yield [14].

Various methods have been applied for the removal of pollutants from wastewater [15,16]. It has been proven to be easy, effective, and efficient to use porous carbon as an adsorbent to remove pollutants. Recent environmental research has concentrated on inexpensive alternative adsorbents since commercially activated carbons are still expensive to obtain and regenerate. Natural materials and waste products from industry and agriculture have all been well-researched [7,17].

Carbonization temperature, impregnation ratio, and activation time are important parameters in the manufacture of porous carbon with a high BET surface area and yield [3]. It is critical to use an experimental design to assess the effects of these factors on the prepared activated carbon. Many researchers used surface response methodology (RSM) to investigate the interactions of two or more parameters [18]. The optimal experimental conditions in a variety of processes, including the production of porous carbon, can be determined. The RSM is a vital tool for reducing the number of experimental runs while still retaining enough information to produce statistically acceptable results [19].

However, in recent years, the industrial production of activated carbon has faced the problem of raw material scarcity and high cost, resulting in its price rising and limiting its use in pollutant treatment. As a result, it has become a focus of current research to look for low-cost raw materials to reduce the cost of producing activated carbon. In this study, Noug stalk was selected as an adsorbent due to its wider accessibility and low cost as compared with some other types of adsorbents studied before. Previously studied adsorbents for treating wastewater, such as teff stalk [20], maize stalk & tassel [7,8], rice husk [9], and sunflower stalk [10], have cost & availability issues for large-scale industrial use, as they are used for animal feed & other purposes, and they are not produced in all parts of the country. Noug is a major source of edible seed oil in Ethiopia [21]. The vegetable seed oil from Noug adds significant economic and nutritional value to the country and its people, and it is regarded as the best seed oil among Ethiopians [22]. Noug Seed is one of the exported commodities that contributes to the generation of hard currency for the country [22]. Its production accounts for 50–60% of Ethiopia's edible oil requirements [23]. Moreover, the rising number of oil-producing factories in Ethiopia may lead to an extra increment of large-scale Noug cultivation soon [24]. This implies that it produces more agro-waste and makes it more accessible. Therefore, Noug stalk would be much more readily available than it is now.

Also, materials containing lignocellulose is a high-grade precursor for preparing activated carbon due to its high carbon content (usually above 45%) [25,26], and, agricultural and wood wastes mainly the shell or stones, stalk or straw, like Noug stalk in this study are used. As far as our review there is no study conducted for evaluating the application of Noug stalk for preparing an activated carbon. Noug stalk has no value for animal feeding and other pertinent purposes; it is a low-cost agro-waste that is readily available in the field. As a result, the main aim of this study was to prepare a low-cost Noug stalk-activated carbon at optimized process conditions using an agro-waste Noug stalk. The impacts of a preliminary carbonization temperature, impregnation ratio with phosphoric acid, and activation time on the activated carbon properties were studied.

## 2. Experimental method

### 2.1. Production of Noug stalk-based activated carbon

Noug stalks were obtained from farmers and local markets. The dirt and materials found on the raw Noug stalk's surface were washed away. The Noug stalk was then sundried and grounded into a powder, and 100 g of Noug stalk powder was impregnated with three different ratios of 1:1, 1:2, and 1:3 with concentrated phosphoric acid (85% w/w) for 24 h. Then the impregnated residue was washed with distilled water until it reached neutral pH and then soaked overnight in a 2%  $NaHCO_3$  solution to remove excess acid. The product was also air-dried at room temperature. Then the product was put in an oven at 105 °C for another 24 h. The oven-dried sample was placed in a dry, known-weight crucible, which was then placed in a rectangular furnace (model F 330, UK). Carbonization was performed at three different temperature levels: 450 °C, 550 °C, and 650 °C, with three different activation times: 90 min, 120 min, and 150 min. The effect of each studied parameter was examined by considering the surface area and yield as response variables. For a while, the carbonized activated carbon was held in a desiccator. Then it was grounded in a mortar and sieved in the 1–2 mm range [27]. Finally, the NSAC was packed in airtight plastic bags for future use in the adsorption process.

## 2.2. Design of the experiment

The current study uses a standard central composite design (CCD) in RSM to better understand the combined influence of constraints in the production of NSAC. The CCD is a popular modeling and optimization method because it needs a small number of experiments to analyze the effect of many process parameters and predict the optimized condition. The CCD is comprised of three different types of runs: factorial ( $2^n$ ), axial ( $2n$ ), and center runs ( $n_c$ ), where  $n$  denotes the number of variables [28]. The center points are intended to reduce experimental error and increase data reproducibility [14]. As a result, the number of experimental runs necessary has increased [29] as given by Eq. (1):

$$N = 2^n + 2n + n_c \quad (1)$$

Carbonization temperature (a), impregnation ratio (b), and activation time (c) are the three variables [30–32] employed in this investigation. Preliminary and literature studies led to the selection of these three important parameters and their respective ranges (see Table 1). We are also limited to these parameters due to the feasibility of the study. As a result, the number of center runs was six for three parameters. The experimental runs required for this study were computed as:

$$N = 2^n + 2n + n_c = 2^3 + 2(3) + 6 = 20$$

This required 20 exploratory runs, which included 8 factorial runs, 6 axial runs, and 6 center runs. The surface area and yield of the prepared activated carbon are the response variables used in this study.

## 2.3. Statistical analysis and modeling

The experimental design for optimizing the production of porous carbon using Noug stalk and the statistical analysis was performed using RSM via face-centered CCD. Design expert (Stat-Ease, Inc., version 7.0) software. The BET surface area and yield of porous carbon were entered as a response in the design layout. The statistical analysis that was performed included generation and fitness testing of the model and ANOVA analysis. A model was chosen based on P-value (P-value < 0.01), lack of fit (P > 0.01) and R-square near to linearity. The effect of each process variable and its interaction with the outcome variable was evaluated by ANOVA. The significance level of 0.01 was used to evaluate whether the process parameter had a significant effect on the response variables or not. Multiple linear regression was employed to assess the magnitude and direction of the effect of each process variable [carbonization temperature (A), impregnation ratio (B), and activation time (C)] and their interaction with the BET surface area ( $Y_1$ ) and yield ( $Y_2$ ) of NSAC. The significance of each coefficient was determined using the P-value. The lower the P-value, the greater the significance of the resulting coefficient. The model with an R-Squared approach to linearity ( $R^2 = 1$ ) was selected as the best model to explain the preparation of activated carbon using the Noug stalk.

## 2.4. Characterization of prepared porous carbon

After the optimal conditions of carbonization temperature, impregnation ratio, and activation time were identified, porous carbon was prepared and characterized through proximate analysis and physicochemical analysis using standard methods developed by the American Society for Testing and Materials (ASTM) (Table 2). The surface functional group of the adsorbent and its importance in adsorption were also investigated using an FT-IR-65 (Fourier transform infrared) Spectrometer in the 400–4000  $\text{cm}^{-1}$  range. Under optimized conditions, the nitrogen adsorption-desorption isotherm was also used to determine the textural properties of prepared activated carbon.

### 2.4.1. BET surface area determination

Brunauer-Emmet-Teller (BET) isotherm equations were used to determine the surface area of raw and porous carbon. The analysis was carried out on the Micromeritics ASAP 2020 surface area analyzer at  $-195.79$  °C. The samples were degassed at 90 °C for 1 h and 350 °C for 4 h, respectively [19]. The materials removed initially were degassed in the first stage, while the remaining adsorbed materials that distort the reading on the microporous sample were degassed in the second stage.

### 2.4.2. Yield of activated carbon

It expresses the amount of carbon that can be produced to the amount of raw material used. Both  $W_o$  and  $W_{AC}$  were determined using an analytical balance, and the carbon yield was calculated as in Eq. (2):

**Table 1**  
The range of process parameters used in the production of porous carbon.

Parameters to be studied	Range of parameters			References
	−1	0	+1	
Carbonization temperature (°C)	450	550	650	[33,34]
Impregnation ratio (w/w)	1:1	1:2	1:3	[35,36]
Activation time (min.)	90	120	150	[3,19]

**Table 2**  
Standard methods applied to determine the characteristics of NSAC.

Characteristics of NSAC	Standard methods used	References
Moisture content	ASTM D2867-99	[37]
Ash content	ASTM D2866-94	[38]
Volatile matter	ASTM D5832-95	[27]
Yield	–	[39]
Iodine number	ASTM D4607-94	[40]
Fixed carbon	–	[41]
Bulk density and porosity	ASTM D2854-96	[27]
pH	ASTM D3838-80	[42]
Point of zero charge	Solid addition method	[41]

$$Y_c = W_{AC}/W_O \times 100 \quad (2)$$

where:  $W_O$  – dry weight before chemical impregnation and  $W_{AC}$  – the dry weight of produced Noug stalk porous carbon.

### 3. Results and discussion

#### 3.1. Designs of experiments for the production of activated carbon

With 20 random experimental runs, the interaction effect of three examined variables, carbonization temperature (A), impregnation ratio (B), and activation time (C) on the surface area and yield of prepared porous carbon was investigated. Table 3 showed that the surface area and yield of porous carbon were calculated using a surface area analyzer and calculated after the activation process, respectively. The surface area of activated carbon varied between 265.34 m<sup>2</sup>/g and 455.01 m<sup>2</sup>/g. The yield of porous carbon, on the other hand, ranged from 18.76% to 57.78%.

#### 3.2. Activated carbon preparation process parameter modeling and model analysis

The model selection was done using the Design of expert response surface approach and CCD. The model was chosen based on the values of adjusted and predicted R-Squared values obtained from the output of various RSM-CCD summary statistics (Tables 4 and 5). Both responses were suggested with a quadratic model based on the sequential model sum of squares. According to the model summary statistics (Table 4) for the surface area of porous carbon, the quadratic model was the highest order polynomial function with the highest R-Squared value of (0.920), a significant model (p-value = 0.001), and an insignificant lack of fitness (p-value = 0.996).

For the yield of porous carbon quadratic model was the highest order polynomial with the highest R-squared value of 0.891, and a significant model (p-value < 0.001). As a result, the quadratic model was chosen as the optimum model for representing the production of porous carbon from the Noug stalk. This is also in line with the other studies conducted [14,19].

The final empirical models for surface area (Y1) and carbon yield (Y2) in terms of coded factors are shown in Equations (3) and (4),

**Table 3**  
CCD matrix for the experimental design and the response for surface area and yield of activated carbon.

Run	A: Carbonization temperature (°C)	B: Impregnation ratio (1:x)	C: Activation time (min.)	Surface area (m <sup>2</sup> /g) (Y1)			Yield (%) (Y2)		
				Actual	Predicted	Residual	Actual	Predicted	Residual
1	450.00	3.00	90.00	342.21	341.99	0.22	43.40	43.04	0.36
2	450.00	3.00	150.00	367.10	367.54	-0.44	23.52	23.43	0.09
3	650.00	3.00	90.00	318.40	318.09	0.31	18.76	18.61	0.15
4	450.00	1.00	150.00	402.03	402.45	-0.42	31.87	31.65	0.22
5	550.00	2.00	120.00	431.56	431.92	-0.36	56.29	56.45	-0.16
6	650.00	1.00	90.00	376.03	376.34	-0.31	21.24	21.04	0.20
7	550.00	2.00	120.00	455.01	455.32	-0.31	54.40	54.71	0.02
8	550.00	2.00	120.00	441.30	441.80	-0.50	56.43	56.13	0.30
9	550.00	0.32	120.00	271.90	271.67	0.23	43.19	43.56	-0.37
10	550.00	3.68	120.00	297.43	297.43	0.00	32.85	32.54	0.31
11	650.00	3.00	150.00	386.10	386.54	-0.44	44.26	44.07	0.19
12	550.00	2.00	69.55	291.30	291.91	-0.61	37.81	37.45	0.36
13	381.82	2.00	120.00	416.87	416.37	0.50	27.29	27.57	-0.28
14	550.00	2.00	120.00	439.12	439.52	-0.40	50.50	50.87	-0.37
15	550.00	2.00	120.00	453.21	453.61	-0.40	53.91	53.73	0.18
16	718.18	2.00	120.00	287.30	287.60	-0.30	34.13	34.54	-0.41
17	550.00	2.00	170.45	371.80	372.20	-0.40	19.76	20.20	-0.44
18	550.00	2.00	120.00	449.50	449.32	0.18	57.78	57.26	0.52
19	650.00	1.00	150.00	345.89	345.56	0.33	46.09	46.34	-0.25
20	450.00	1.00	90.00	265.34	265.06	0.28	27.34	27.12	0.22

**Table 4**  
Model summary statistics for the surface area of the prepared porous carbon.

Model summary statistics					
Source	Std.Dev	R-Squared	Adjusted R-Squared	Predicted R-Squared	
Linear	8.45	0.130	-0.032	-0.291	
2FI	9.58	0.160	-0.226	-1.096	
Quadratic	<b>3.05</b>	<b>0.920</b>	<b>0.908</b>	<b>0.915</b>	<b>Suggested</b>
Cubic	27.46	0.826	0.901		<b>Aliased</b>

**Table 5**  
Model summary statistics for the yield of the prepared porous carbon.

Model summary statistics					
Source	Std. DeV	R-Squared	Adjusted R-Squared	Predicted R-Squared	
Linear	14.60	0.012	-0.172	-0.520	
2FI	14.63	0.194	-0.177	-1.523	
Quadratic	<b>8.35</b>	<b>0.912</b>	<b>0.891</b>	<b>0.870</b>	<b>Suggested</b>
Cubic	2.43	0.826	0.901	0.837	<b>Aliased</b>

respectively.

$$Y_1 = +444.20 - 6.72 * A + 6.11 * B + 25.67 * C - 5.42 * A * B - 13.50 * A * C - 3.75 * B * C - 18.21 * A^2 - 51.75 * B^2 - 35.17 * C^2 \quad (3)$$

$$Y_2 = +54.91 + 1.15 * A - 1.02 * B - 0.89 * C - 1.50 * A * B + 8.21 * A * C - 2.97 * B * C - 8.73 * A^2 - 6.14 * B^2 - 7.64 * C^2 \quad (4)$$

In the above equation, signs in front of the terms denote whether they have a synergistic (plus) effect or an antagonistic (minus) effect upon the outcome variables.

### 3.2.1. ANOVA analysis

The ANOVA test was used to investigate the significant effect of the individual components and their interactions on the surface area characteristics of the prepared porous carbon. Based on the ANOVA for the response surface quadratic model for surface area, the model F-value of 1021.35 indicated that it was significant. Significant model terms had P-values of less than 0.050. In this study, the model terms A, B, C, AB, BC, A<sup>2</sup>, B<sup>2</sup>, and C<sup>2</sup> were significant. The values of all three parameters (carbonization temperature, impregnation ratio, and activation time) are much less than 0.05, as shown by the p-values of the model coefficients in Table 6. This means that all of the process parameters are more important to the characteristics of the prepared activated carbon.

Table 7 displays the ANOVA for the quadratic model of porous carbon yield. The model has a significant F-value of 6.77. A, AC, A<sup>2</sup>, B<sup>2</sup>, and C<sup>2</sup> were important model terms in this case. According to the statistical results, the quadratic model was appropriate for predicting surface area and yield within the range of parameters studied.

Figures S1 and S2 (Appendix) show the residual normality plots for surface area and yield of porous carbon, respectively. As all of the points are close to the diagonal line, it indicates that the errors are normally distributed. To investigate the effect of outliers and

**Table 6**  
ANOVA for quadratic model: response 1: surface area, transform: square root.

Source	Sum of squares	Df	Mean square	F value	p-value Prob > F	
Model	1866.19	14	133.30	1021.35	<0.001	Significant
A-Carbonization temperature	16.44	1	16.44	104.96	0.001	Significant
B-Impregnation ratio	50.00	1	50.00	95.52	<0.016	Significant
C-Activation time	5.05	1	5.05	24.59	0.048	Significant
AB	0.12	1	0.12	90.11	0.010	Significant
AC	1.23	1	1.23	1.12	0.062	Not Significant
BC	19.98	1	19.98	180.19	0.007	Significant
A <sup>2</sup>	121.88	1	121.88	910.95	<0.001	Significant
B <sup>2</sup>	67.15	1	67.15	617.13	<0.001	Significant
C <sup>2</sup>	18.12	1	18.12	169.49	0.001	Significant
Lack of fit	1.55	9	0.17	0.05	0.996	Not Significant
Pure error	14.93	6	1.76			

**Table 7**  
ANOVA for quadratic model: response 2: yield of activated carbon, transform: none.

Source	Sum of squares	df	Mean square	F value	p-value	Prob > F
Model	2906.88	9	322.99	6.77	0.003	Significant
A-Activation temperature	18.10	1	18.10	4.38	0.001	Significant
B-Impregnation ratio	14.33	1	14.33	0.30	0.595	Not Significant
C-Activation time	1.58	1	1.58	0.03	0.859	Not Significant
AB	18.06	1	18.06	0.38	0.552	Not Significant
AC	539.56	1	539.56	11.32	0.007	Significant
BC	70.57	1	70.57	1.48	0.251	Not Significant
A <sup>2</sup>	1005.89	1	1005.89	21.09	0.001	Significant
B <sup>2</sup>	479.81	1	479.81	10.06	0.010	Significant
C <sup>2</sup>	1176.46	1	1176.46	24.67	0.006	Significant
Lack of fit	443.70	5	88.74	13.38	0.641	Not Significant
Pure error	33.16	5	6.63			

satisfaction with the analysis of variance assumptions, different diagnostic and influence graphs (actual vs predicted plot, leverage, DFFITS, DFBETAS, and Cooks distance plots) were used. All of the plots demonstrated that the model met the ANOVA assumption (See Annex 1).

3.3. Estimation of quantitative effects of the factors upon the surface area and yield of prepared porous carbon

The CCD approach is used to assess the effect of a process variable on the outcome variable. The effect of interacting two parameters at a time on the response was examined and illustrated below using 3D response surface plots while holding other variables constant.

3.3.1. Combined effect of carbonization temperature and impregnation ratio

As shown in Fig. 1, the combined effect of carbonization temperature and impregnation ratio was examined at a constant activation time (120 min). The BET surface area of porous carbon is increased as the carbonization temperature is increased from 450 °C to 550 °C, but it begins to drop as the carbonization temperature increases from 550 °C to 650 °C. This might be because the carbonized materials and activator react slowly at lower temperatures, which is unfavorable for pore formation, but the higher temperatures likely resulted in the melting of micro-pores generated earlier in the process [43]. The phenomenon was consistent with previous research [43]. The surface area of porous carbon increases as the impregnation ratio increases from 1:1 to 1:2, but it begins to drop as the impregnation ratio increases from 1:2 to 1:3. This could be owing to a lack of fresh micropore development and the conversion of existing micropores to mesopores [44]. This result is in close agreement with previous studies [45,46].

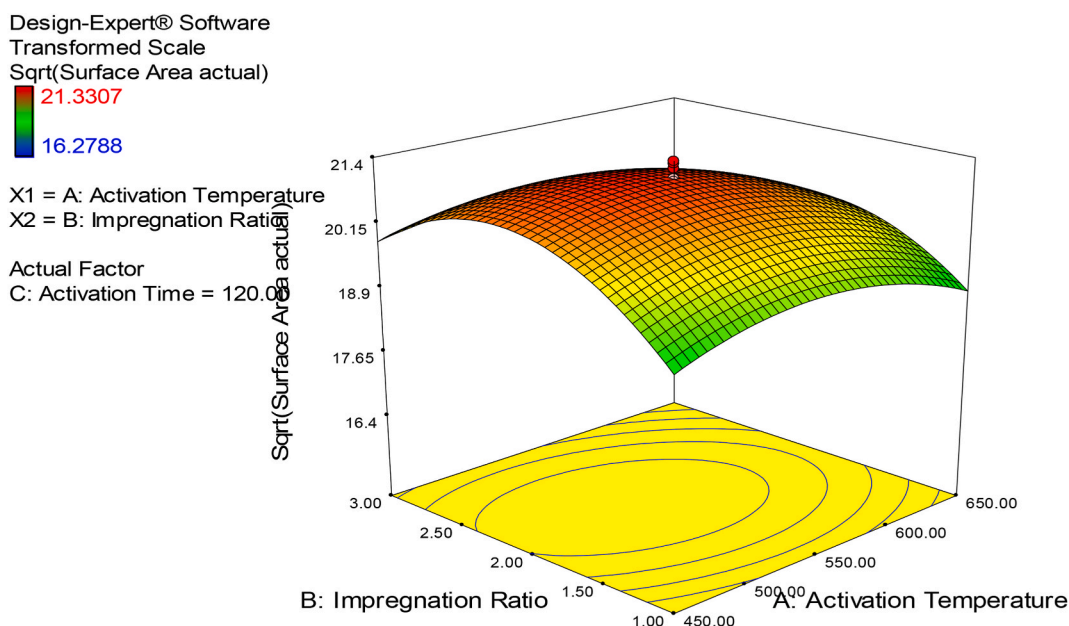


Fig. 1. Effect of interaction between carbonization temperature and impregnation ratio on the surface area of porous carbon-response surface plot.

### 3.3.2. Combined effect of impregnation ratio and activation time

As shown in Fig. 2, the combined effect of the impregnation ratio and activation time was examined at a constant carbonization temperature (550 °C). The surface area of porous carbon is increased as the impregnation ratio is increased from 1:1 to 1:2, but it begins to drop as the impregnation ratio increases. The surface area of porous carbon increases as the activation time increases from 90 min to 120 min, but it begins to drop as the activation time increases beyond 120 min. It has a significant effect on the surface area of activated carbon with a p-value of 0.0007 (Table 5). From Fig. 5, the maximum surface area at all the studied activation times takes place at an impregnation ratio of 2 and an activation time of 120 min. This could be because as the activated carbon is prepared, the activating agent and activator have more time to build a pore. The best period is 120 min since a long time (>120 min) may destroy the previously produced microporous structure, while a shorter time (120 min) cannot enrich the production of micropores and mesopores [43]. This finding is in line with the findings of previous research [45].

### 3.3.3. Combined effect of carbonization temperature and activation time

Fig. 3 depicts the variation in porous carbon yield as a function of carbonization temperature and activation time in the form of a 3D surface plot. At temperatures above 550 °C, the yield decreases significantly, whereas the variation in yield to activation time is comparatively less significant (see Table 7) at higher carbonization temperatures than at lower carbonization temperatures. An increase in carbonization temperature and activation time speeds up the C-CO<sub>2</sub> reaction, resulting in a lower yield.

### 3.4. Optimum condition for the preparation of activated carbon

After examining the effects of all interactions between the process parameters, Design Expert version 7.0.0 software was used to optimize the activated carbon preparation process. The point optimization was carried out as shown in Table 8, and the best potential operating conditions with the highest desirability, surface area, and yield were chosen. The software looked for a combination of characteristics that met the requirements of maximum surface area, yield, and highest desirability at the same time. Table 9 shows, the optimum settings (carbonization temperature, impregnation ratio, and activation time) that offer the maximum composite desirability (1.0), surface area (473.45 m<sup>2</sup>/g), and yield (53.78%) from the Design Expert software.

### 3.5. Characterization of produced Noug stalk activated carbon

The physico-chemical characteristics of NSAC (Table 10) show that the produced porous carbon has an excellent quality to be used as an adsorbent.

#### 3.5.1. Moisture content, volatile matter, and ash content

One of the most essential characteristics for determining the compactness of activated carbon is its ash content. It is a measure of porosity and strength. An adsorbent with a lower ash percentage is less compacted and more porous, and vice versa [42]. As shown in Table 10, the ash content of NSAC was found to be 8% in this study. The produced NSAC is very porous, indicating that it can be employed as an effective adsorbent for the removal of heavy metals from an aqueous solution. This could be due to the Noug stalk's lower inorganic content [47]. The lower volatile matter concentration of NSAC could be attributable to the precursor's lower non-carbonaceous matter composition [48]. The hydrophobic nature of the manufactured activated carbon may account for the lower

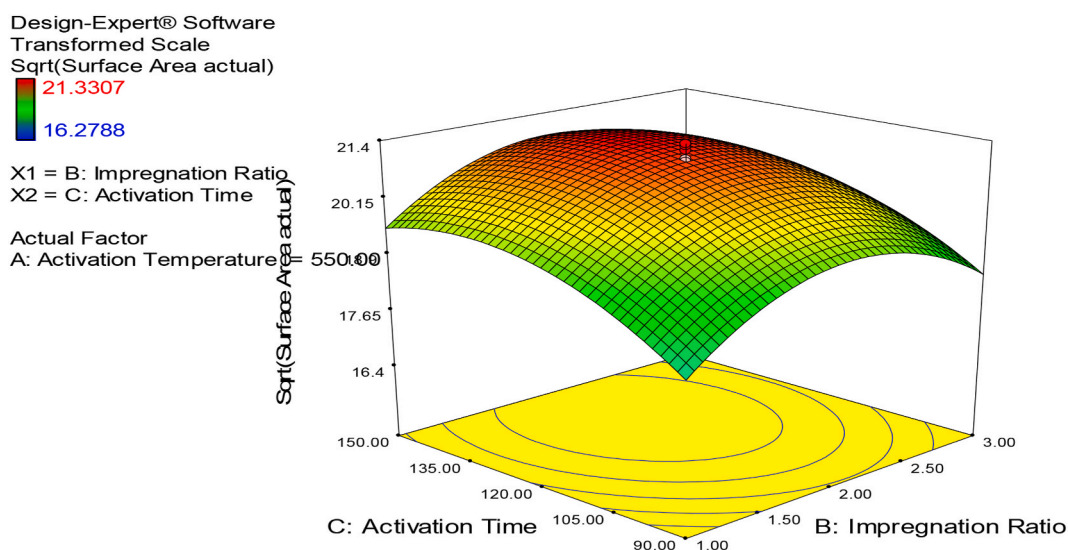


Fig. 2. Effect of interaction between impregnation ratio and activation time on the surface area of the activated carbon-response surface plot.

Design-Expert® Software

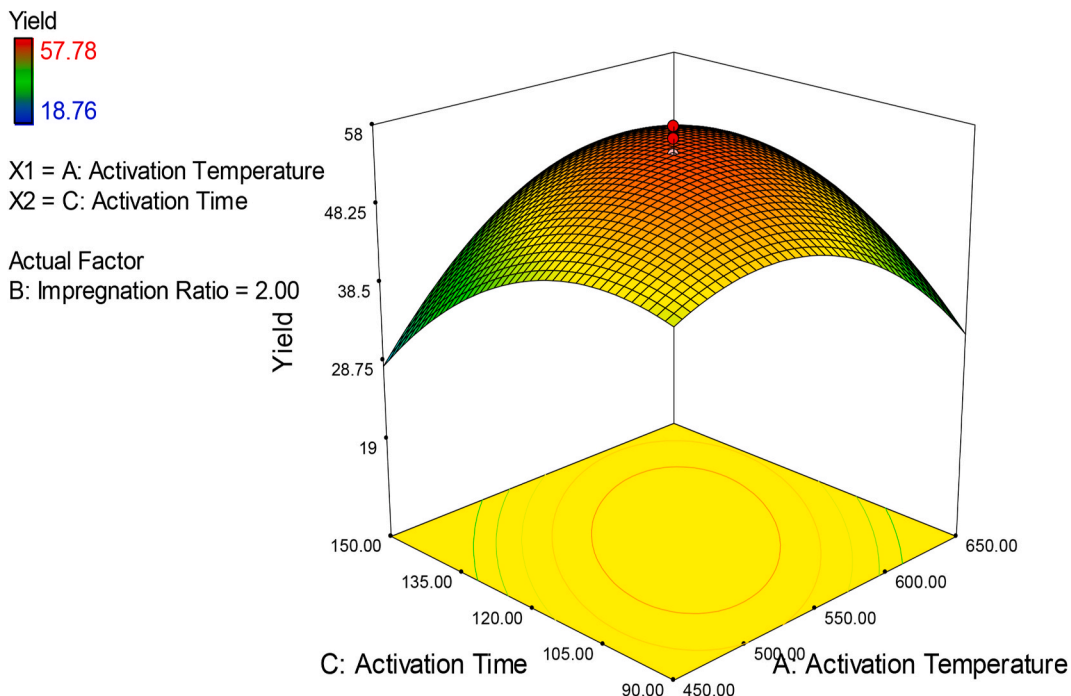


Fig. 3. Effect of interaction between carbonization temperature and activation time on the yield of porous carbon-response surface plot.

Table 8

Working conditions of response and factors for optimization.

Name	Goal	Lower limit	Upper limit	Lower weight	Upper weight	Importance
A: Carbonization temperature (°C)	in range	450	650	1	1	3
B: Impregnation ratio (1:X)	in range	1	3	1	1	3
C: Activation time (min.)	in range	90	150	1	1	3
Surface area (m <sup>2</sup> /g)	Maximize	265.34	455.01	1	1	3
Yield (%)	Maximize	18.76	57.78	1	1	3

Table 9

Optimum condition with maximum surface area and yield of prepared porous carbon.

No.	Carbonization temperature (°C)	Impregnation ratio (1:X)	Activation time (min.)	Surface area (m <sup>2</sup> /g)	Yield (%)	Desirability
1	537.50	1.95	127	473.45	53.78	1.00 Selected

Table 10

Physicochemical parameters of Noug stalk activated carbon prepared under optimized conditions.

No.	Characterization	Unit	Value
1	Carbon yield	%	53.78
2	Ash content	%	8.00
3	Fixed carbon	%	55.00
4	Volatile matter content	%	31.00
5	Moisture content	%	6.00
6	Bulk density	g/cm <sup>3</sup>	0.37
7	Porosity	%	67.50
8	BET surface area	m <sup>2</sup> /g	473.45
9	pH	-	6.15
10	Pzc	-	5.43
11	Iodine number	mg/g	576.00

**Table 11**  
Comparison of characteristics of the produced agro-waste-based porous carbon.

AC	Activation method	Characteristics of activated carbon											
		pH	Porosity (%)	CY (%)	FC (%)	MC (%)	AC (%)	VM (%)	BD (g/cm <sup>3</sup> )	Pzc	IN (mg/g)	SA (m <sup>2</sup> /g)	Reference
Noug stalk	Acid activation	6.15	67.50	53.78	55.00	6.00	8.00	31.00	0.37	5.43	576.00	473.45	This work
Corn cob	»	6.20	48.80	55.70	24.80	10.50	1.50	78.20	0.28	–	528.00	–	[50]
Coffee husk	»	5.40	57.30	57.09	71.10	6.30	9.40	13.20	0.69	–	396.00	–	[51]
Maize bran	»	–	37.00	–	31.28	7.97	18.41	42.34	0.24	–	–	437.00	[49]
Maize tassel	»	6.90	–	–	–	0.30	–	–	0.52	–	–	250.00	[8]
Canna Indica	»	–	–	–	62.90	5.40	5.00	26.70	–	–	797.50	–	[55]
Bamboo stem	»	6.40	–	–	62.40	7.60	5.55	24.40	0.65	–	–	–	[56]
Sunflower stalk	»	5.30	–	–	–	–	10.40	–	–	–	–	–	[10]

c

moisture content. This also demonstrated that the produced NSAC's surface is less occupied by water and can be employed as an effective adsorbent for heavy metals in wastewater [49]. As shown in Table 11, the prepared AC has lower ash, volatile matter, and moisture content than some of the porous carbons made from various agricultural wastes.

### 3.5.2. Carbon yield and fixed carbon

Carbon yield is one of the most essential properties of porous carbon, as it determines the feasibility of producing AC from a particular set of precursors [50]. As shown in Table 10, the carbon yield and fixed carbon were found to be 53.78% and 55.00%, respectively. Both findings are supportive of the feasibility of the production of the Noug stalk-activated carbon adsorbent. This value is also higher than the carbon yield of other lignocellulose materials such as coffee husks and corn cob-based porous carbon [50,51].

### 3.5.3. Bulk density, porosity, and surface area

The bulk density of powdered particles is an important variable. According to the American Water Work Association, the bulk density of porous carbon should not be less than 0.25 mg/L for practical application [51]. The bulk density of the prepared NSAC was found to be 0.37 g/cm<sup>3</sup>, which meets the above criteria (Table 10). The bulk density data was also in close agreement with the value reported in the literature for different agro-waste-based activated carbons such as maize bran and corn cob, as shown in Table 11.

The higher surface area of AC is significant since it limits the amount of adsorbate that may be adsorbed. Table 10 shows that the porosity and surface area of the prepared NSAC were 67.50% & 473.45 m<sup>2</sup>/g, respectively. These findings demonstrated that the prepared NSAC was sufficiently porous and had a large surface area. This could be because chemical activation, as opposed to thermal activation, provides increased porosity and surface area in activated carbon [50].

### 3.5.4. pH and point of zero charge determination

The prepared activated carbon has a pH and a Pzc of 6.15 and 5.43, respectively (Table 10). This means that the NSAC's surface will remain positively charged at lower pH levels until the pH hits 5.43. However, as the pH increases, it becomes negatively charged. The presence of acidic functional groups on the surface of NSAC, such as carboxyl, phenolic, and others, could explain the acidic Pzc of manufactured Noug stalk-activated carbon [52]. The Pzc of NSAC was found to be in reasonable agreement with the Pzc of other agro-waste-based activated carbons, according to the data in Table 11.

### 3.5.5. Comparison of physicochemical characteristics of NSAC with other agro-waste-based activated carbons

As seen from Table 11, most of the characteristics of Noug stalk activated carbon were in close agreement with the characteristics of agro waste-based activated carbons such as coffee husk, rice husk, corn cob, and maize bran, and bamboo steam activated carbons. The significant distinction between the properties of other agro-waste activated carbons [17,53,54] prepared for heavy metal removal may be due to the difference in impregnation ratio and carbonization temperature of porous carbon.

### 3.5.6. Fourier transformer infrared (FTIR) spectroscopy analysis

The FT-IR spectrum is a useful tool for identifying the surface functional groups of the produced activated carbon [7]. Many heteroatoms, including oxygen, hydrogen, nitrogen, and others, can be found on the surface of porous carbon as single atoms and/or in the form of functional groups. In the carbon matrix, oxygen is the most dominant heteroatom among several different heteroatoms. The most important centers influencing the surface properties and activities of activated carbon are carbon-oxygen surface compounds [7].

The FTIR analysis was used to look at the organic and inorganic functional groups on the surface of the NSAC that had been prepared. Using KBr pellets, the surface chemistry of porous carbon was investigated using a spectrum 65 FT-IR (PerkinElmer) model in the range of 4000–400 cm<sup>-1</sup>. The IR spectrum was recorded as shown in Fig. 4.

The surface functional groups of NSAC that have been prepared under the optimal preparation conditions were recorded as follows (Table 12).

The presence of hydroxyl (–OH), unsaturated C=C, carboxyl groups, and –C–O–groups on the surface of NSAC was represented by strong peaks in the IR spectra at 3476 cm<sup>-1</sup>, 1640 cm<sup>-1</sup>, 1389 cm<sup>-1</sup>, and 1111 cm<sup>-1</sup>, respectively (Table 12). The spectrum at 3476 cm<sup>-1</sup> may be a phenolic, alcoholic, or carboxylic acid group, which plays a major role in the adsorption process. Similarly, the other spectrums also revealed that the olefin structures (1640 cm<sup>-1</sup>), carboxyl groups (1389 cm<sup>-1</sup>), and secondary hydroxyl functional groups (1111 cm<sup>-1</sup>) on the surface of NSAC might be potential adsorption sites for positively charged heavy metal pollutants from aqueous solution. These functional groups have also been discovered in other porous carbons derived from agricultural waste [7].

### 3.5.7. N<sub>2</sub> adsorption-desorption isotherms

Fig. 5 depicts the nitrogen adsorption-desorption isotherms of activated carbon prepared under optimized process conditions. With a partial pressure (P/P<sub>0</sub>) range of 10<sup>-6</sup> to 1, the nitrogen adsorption-desorption isotherm was measured at 77 K. It can be seen from Fig. 5 that the volume of N<sub>2</sub> adsorbed is increased sharply at lower values of P/P<sub>0</sub> (<0.1), which indicates the filling of micropores, and then reaches a plateau. The adsorption capacity continues to increase with increasing relative pressure up to a P/P<sub>0</sub> value of 1, which is typical of microporous solids with a well-developed mesopore structure.

The Brunauer-Emmett-Teller equation is used to calculate the BET surface area from the nitrogen adsorption-desorption isotherm [57], assuming a 0.16 nm N<sub>2</sub> surface area, and the micropore volume is calculated using the Dubinin-Radushkevich (DR) method [58]. The total volume is estimated by converting the amount of N<sub>2</sub> gas adsorbed at a relative pressure of 0.95 to the equivalent liquid volume of the adsorbate (N<sub>2</sub>) [59].

The BET surface area value of the activated Noug stalk was estimated to be 473.45 m<sup>2</sup>/g, pore volume is estimated to be 0.45 cm<sup>3</sup>/g

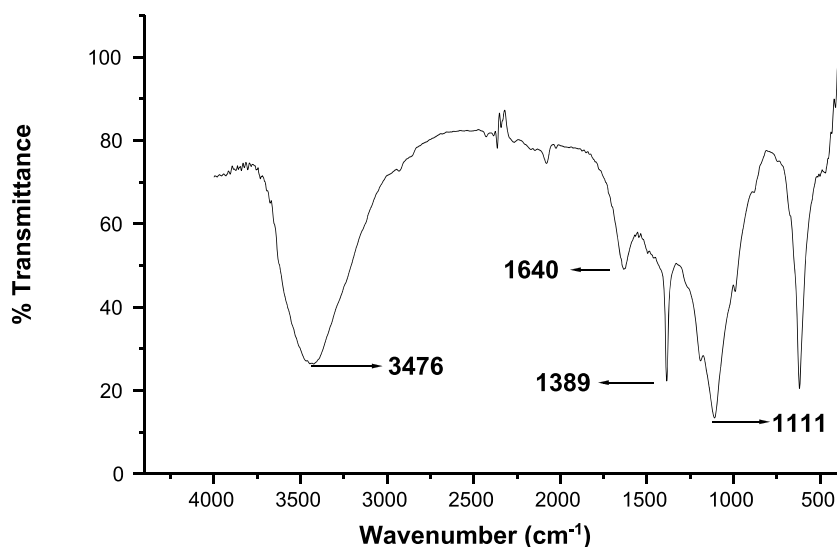


Fig. 4. FT-IR spectra of NSAC in KBr disc that are prepared under the optimal condition.

Table 12

The FT-IR spectra characteristics of the surface of Noug stalk activated carbon.

Wave number (cm <sup>-1</sup> )	Bond	Functional group
3600–3000	Stretching O–H, N–H	Hydroxyl, carboxylic acid
3000–2800	Stretching C–H	Aliphatic, olefinic, and aromatic hydrocarbons
1770–1650	Stretching C=O	Carbonyl
1700–1600	Stretching C=C	Olefin structures
1480–1420	Bending C–H	Aliphatic structure
1430–1360	Bending O–H and C–H	Hydroxyl, carboxylic acid, Olefins, methyl
1120–1070	Stretching C–O	Secondary Hydroxyl

with an average pore size of 1.62 nm (Table 13). The BET surface area was greatly contributed by the micropore surface area ( $S_{\text{micro}}$ ) with a value of 403.26 m<sup>2</sup>/g, and the rest (70.19 m<sup>2</sup>/g) was contributed by the surface area of the mesopores. At temperatures less than 800 °C, the number of micropores is expected to be greater, and hence its surface area is higher [60]. This fact is in line with our reading ( $S_{\text{micro}} > S_{\text{meso}}$ ) since the activation temperature used to produce this activated Noug stalk in this study is below 800 °C. According to the International Union of Pure and Applied Chemistry (IUPAC) notation, the size of the pores for the activated Noug stalk is classified as micropores since the size is less than 2 nm. In general, micropores with a higher surface area and volume provide adequate adsorbate storage space, which favors the adsorption of micropollutants [61]. As a result, Noug stalk-activated carbon produced under optimal conditions is predicted to have better properties for use as an adsorbent with high adsorption capacity (Table 13).

#### 4. Limitation of the study

In this study, we used a conventional and widely used method of response surface methodology rather than other options such as orthogonal experiments, which is considered a major strength. Despite the proximate analysis, N<sub>2</sub> adsorption-desorption isotherm, and FT-IR analysis, no elemental or morphological analysis of NSAC including XRD, TGA, EDX/map, SEM, etc., was performed, which could have helped to better understand the characteristics of the produced activated carbon.

#### 5. Conclusion and recommendation

The current study focuses on the production of the Noug stalk porous carbon for an effective and locally available adsorbent for the removal of contaminants such as heavy metal and organic dyes from wastewater. The best conditions for the production of porous carbon are achieved at a carbonization temperature of 537.50 °C, an impregnation ratio of 1.95, and an activation time of 127 min. The quadratic model is the best-fitted model, with an adjusted R-squared value of 0.920 and 0.912 for surface area and yield, respectively. Highly porous NSAC with a surface area of 473.45 m<sup>2</sup>/g is produced at optimal conditions. This porous NSAC can be used as a locally available, low-cost, and environmentally friendly adsorbent for heavy metal removal and organic dyes from contaminated water. Elemental and morphological analysis of NSAC needs to be studied in the future. Moreover, its efficiency in the removal of heavy metal contaminants from wastewater need to be studied in the future.

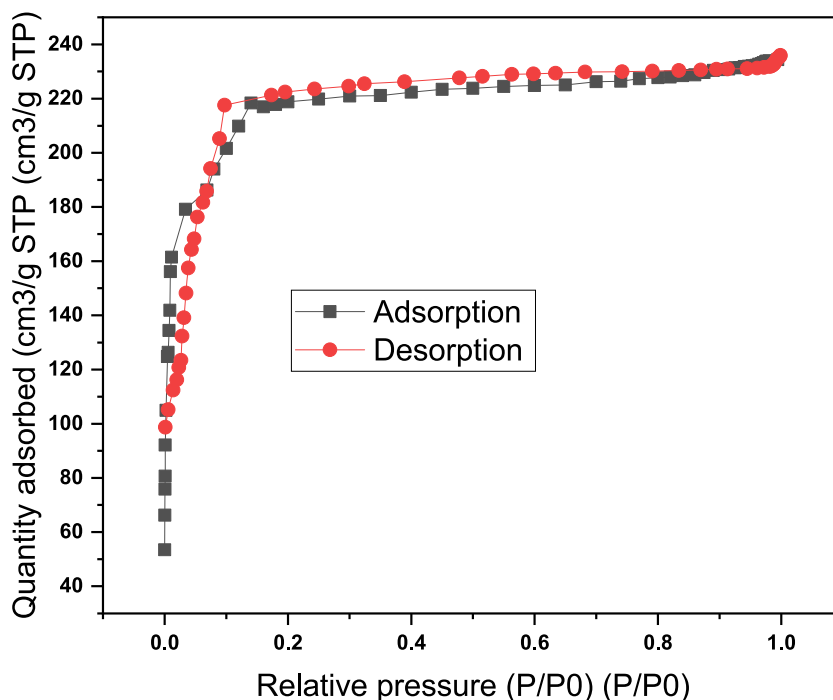


Fig. 5. Nitrogen adsorption-desorption isotherm of the prepared Noug stalk-activated carbon under optimized process conditions.

**Table 13**

Textural properties of Noug stalk-activated carbon obtained by  $N_2$  adsorption-desorption studies.

Type of Noug stalk	Average pore size (nm)	$S_{BET}$ ( $m^2/g$ )	$S_{meso}$ ( $m^2/g$ )	$S_{micro}$ ( $m^2/g$ )	Pore volume ( $cm^3/g$ )		
					$V_{meso}$	$V_{micro}$	Total pores volume
Activated Noug stalk	1.62	473.45	70.19	403.26	0.04	0.41	0.45

**N.B:**  $S_{BET}$  (BET surface area),  $S_{meso}$  (mesopore surface area),  $S_{micro}$  (micropore surface area),  $V_{meso}$  (mesopore volume), and  $V_{micro}$  (micropore volume).

#### Author contribution statement

Getasew Yirdaw, Tsegaye Adane Birhan: Conceived and designed the experiments; Performed the experiments; Analyzed and interpreted the data; Contributed reagents, materials, analysis tools or data; Wrote the paper.

Awrajaw Dessie: Conceived and designed the experiments; Analyzed and interpreted the data; Contributed reagents, materials, analysis tools or data; Wrote the paper.

#### Data availability statement

Data included in article/supplementary material/referenced in article.

#### Declaration of competing interest

The authors declare that they have no known competing financial interests or personal relationships that could have appeared to influence the work reported in this paper.

#### Acknowledgements

The authors would like to acknowledge Debre Markos University for allocating a fund for this study. Also, our appreciation goes to the University of Gondar, Environmental and Occupational Health and Safety Department staff, for their cooperative and constructive roles for the betterment of this study.

## Appendix. ASupplementary data

Supplementary data related to this article can be found at <https://doi.org/10.1016/j.heliyon.2023.e17254>.

## Supplementary Material

Annex 1: shows the residual normality plots for surface area and yield of porous carbon. Figure S1 depicts the graph of normal% probability vs. internally studentized residual for surface area. The figure shows that all residual points are close to the diagonal line, which means that the errors are normally distributed. Figure S2 depicts a graph of normal% probability vs. internally studentized residual for porous carbon yield. All of the residual points in the diagram are close to the diagonal line, indicating that the errors are normally distributed.

## References

- [1] Z. Heidarinejad, et al., Methods for preparation and activation of activated carbon: a review, *Environ. Chem. Lett.* 18 (2020) 393–415.
- [2] Z. Belala, et al., Biosorption of basic dye from aqueous solutions by date stones and palm-trees waste: kinetic, equilibrium and thermodynamic studies, *Desalination* 271 (1–3) (2011) 80–87.
- [3] O. Üner, Y. Bayrak, The effect of carbonization temperature, carbonization time and impregnation ratio on the properties of activated carbon produced from *Arundo donax*, *Microporous Mesoporous Mater.* 268 (2018) 225–234, <https://doi.org/10.1016/j.micromeso.2018.04.037>.
- [4] B. Corcho-Corral, et al., Preparation and textural characterisation of activated carbon from vine shoots (*Vitis vinifera*) by H<sub>3</sub>PO<sub>4</sub>—chemical activation, *Appl. Surf. Sci.* 252 (17) (2006) 5961–5966, <https://doi.org/10.1016/j.apsusc.2005.11.007>.
- [5] F.-C. Wu, R.-L. Tseng, R.-S. Juang, Preparation of highly microporous carbons from fir wood by KOH activation for adsorption of dyes and phenols from water, *Sep. Purif. Technol.* 47 (1–2) (2005) 10–19, <https://doi.org/10.1016/j.seppur.2005.03.013>.
- [6] A.L. Ayele, B.Z. Tizazu, A.B. Wassie, Chemical modification of teff straw biomass for adsorptive removal of Cr (VI) from aqueous solution: characterization, optimization, kinetics, and thermodynamic aspects, *Adsorpt. Sci. Technol.* 2022 (2022).
- [7] G. García-Rosales, A. Colín-Cruz, Biosorption of lead by maize (*Zea mays*) stalk sponge, *J. Environ. Manag.* 91 (11) (2010) 2079–2086, <https://doi.org/10.1016/j.jenvman.2010.06.004>.
- [8] M. Moyo, et al., Adsorption batch studies on the removal of Pb (II) using maize tassel based activated carbon, *J. Chem.* 2013 (2013), <https://doi.org/10.1155/2013/508934>.
- [9] H. Amer, A. El-Gendy, S. El-Haggag, Removal of lead (II) from aqueous solutions using rice straw, *Water Sci. Technol.* 76 (5) (2017) 1011–1021, <https://doi.org/10.2166/wst.2017.249>.
- [10] M. Jalali, F. Aboughazi, Sunflower stalk, an agricultural waste, as an adsorbent for the removal of lead and cadmium from aqueous solutions, *J. Mater. Cycles Waste Manag.* 15 (4) (2013) 548–555, <https://doi.org/10.1007/s10163-012-0096-3>.
- [11] A. Nayak, et al., Chemically activated carbon from lignocellulosic wastes for heavy metal wastewater remediation: effect of activation conditions, *J. Colloid Interface Sci.* 493 (2017) 228–240.
- [12] A. Ahmadpour, D. Do, The preparation of activated carbon from macadamia nutshell by chemical activation, *Carbon* 35 (12) (1997) 1723–1732, [https://doi.org/10.1016/S0008-6223\(97\)00127-9](https://doi.org/10.1016/S0008-6223(97)00127-9).
- [13] I. Okman, et al., Activated carbons from grape seeds by chemical activation with potassium carbonate and potassium hydroxide, *Appl. Surf. Sci.* 293 (2014) 138–142.
- [14] K. Patidar, M. Vashishtha, Optimization of process variables to prepare mesoporous activated carbon from mustard straw for dye adsorption using response surface methodology, *Water Air Soil Pollut.* 231 (10) (2020) 1–17.
- [15] W.N.W. Ismail, et al., Adsorption behavior of heavy metal ions by hybrid inulin-TEOS for water treatment, *Civ. Eng. J.* 8 (9) (2022) 1787–1798.
- [16] C. Peña-Guzmán, B.E. Ortiz-Gutierrez, Evaluation of three natural coagulant from moringa oleifera seed for the treatment of synthetic greywater, *Civ. Eng. J.* 8 (12) (2022) 3842–3853.
- [17] R. Suzuki, et al., Preparation and characterization of activated carbon from rice bran, *Bioresour. Technol.* 98 (10) (2007) 1985–1991, <https://doi.org/10.1016/j.biortech.2006.08.001>.
- [18] R. Ratnawati, Response Surface Methodology for Formulating PVA/Starch/Lignin Biodegradable Plastic, 2022.
- [19] N.S. Sulaiman, et al., Optimization of activated carbon preparation from cassava stem using response surface methodology on surface area and yield, *J. Clean. Prod.* 198 (2018) 1422–1430, <https://doi.org/10.1016/j.jclepro.2018.07.061>.
- [20] J. Simon, Adsorption of Pb (II) from Aqueous Solution Solution onto Microwave and Conventional Method Prepared Activated Carbon from Teff Husk Using ZnCl<sub>2</sub> as an Activated Agent, 2018.
- [21] S. Tsehay, et al., Nutritional profile of the Ethiopian oilseed crop noug (*Guizotia abyssinica* cass.): opportunities for its improvement as a source for human nutrition, *Foods* 10 (8) (2021) 1778.
- [22] A. Tesfaye, et al., Production, Marketing, Processing and Technology Adoption of Noug (*Guizotia Abyssinica*) in Central Ethiopia, *Ethiopian Institute of Agricultural Research (EIAR)*, 2016.
- [23] G. Alemaw, A.T. Wold, Noug breeding in Ethiopia, in: *First National Oilseeds Workshop, Addis Abeba (Ethiopia)*, IAR, 1992, 3–5 Dec 1991.
- [24] J. Wijjandans, J. Biersteker, E. Van Loo, Oilseeds Business Opportunities in Ethiopia 2009, PPP, 2009.
- [25] J. Alcañiz-Monge, M.D.C. Román-Martínez, M. Lillo-Ródenas, Chemical activation of lignocellulosic precursors and residues: what else to consider? *Molecules* 27 (5) (2022) <https://doi.org/10.3390/molecules27051630>.
- [26] J. Saleem, et al., Production and applications of activated carbons as adsorbents from olive stones, *Biomass Convers. Biorefin.* 9 (4) (2019) 775–802, <https://doi.org/10.1007/s13399-019-00473-7>.
- [27] T. Adane, et al., Response surface methodology as a statistical tool for optimization of removal of chromium (VI) from aqueous solution by Teff (*Eragrostis teff*) husk activated carbon, *Appl. Water Sci.* 10 (1) (2020) 1–13, <https://doi.org/10.1007/s13201-019-1120-8>.
- [28] K. Cronje, et al., Optimization of chromium (VI) sorption potential using developed activated carbon from sugarcane bagasse with chemical activation by zinc chloride, *Desalination* 275 (1–3) (2011) 276–284, <https://doi.org/10.1016/j.desal.2011.03.019>.
- [29] M. Arulkumar, P. Sathishkumar, T. Palvannan, Optimization of Orange G dye adsorption by activated carbon of *Thespesia populnea* pods using response surface methodology, *J. Hazard Mater.* 186 (1) (2011) 827–834, <https://doi.org/10.1016/j.jhazmat.2010.11.067>.
- [30] J. Tay, et al., Optimising the preparation of activated carbon from digested sewage sludge and coconut husk, *Chemosphere* 44 (1) (2001) 45–51.
- [31] G. Stavropoulos, A. Zabaniotou, Production and characterization of activated carbons from olive-seed waste residue, *Microporous Mesoporous Mater.* 82 (1–2) (2005) 79–85.
- [32] Y. Sudaryanto, et al., High surface area activated carbon prepared from cassava peel by chemical activation, *Bioresour. Technol.* 97 (5) (2006) 734–739.

- [33] P. Foo, L. Lee, Preparation of activated carbon from parkia speciosa pod by chemical activation, in: Proceedings of the World Congress on Engineering and Computer Science, Citeseer, 2010.
- [34] M. Dizbay-Onat, U.K. Vaidya, C.T. Lungu, Preparation of industrial sisal fiber waste derived activated carbon by chemical activation and effects of carbonization parameters on surface characteristics, *Ind. Crop. Prod.* 95 (2017) 583–590.
- [35] O. Olorundare, et al., Potential application of activated carbon from maize tassel for the removal of heavy metals in water, *Phys. Chem. Earth, Parts A/B/C* 50 (2012) 104–110, <https://doi.org/10.1016/j.pce.2012.06.001>.
- [36] V. Gómez-Serrano, et al., Preparation of activated carbons from chestnut wood by phosphoric acid-chemical activation. Study of microporosity and fractal dimension, *Mater. Lett.* 59 (7) (2005) 846–853.
- [37] D. Olowoyo, E. Orere, Preparation and characterization of activated carbon made from palm-kernel shell, coconut shell, groundnut shell and obeche wood (investigation of apparent density, total ash content, moisture content, particle size distribution parameters), *Int. J. Res. Chem. Environ.* 2 (3) (2012) 32–35.
- [38] L.E. Oshido, Meso-microporous Activated Carbon Derived from Raffia Palm Shells: Optimization of Synthesis Conditions Using Response Surface Methodology, 2021, <https://doi.org/10.1016/j.heliyon.2021.e07301>.
- [39] K. Foo, B. Hameed, Factors affecting the carbon yield and adsorption capability of the mangosteen peel activated carbon prepared by microwave assisted K<sub>2</sub>CO<sub>3</sub> activation, *J. Chem. Eng.* 180 (2012) 66–74.
- [40] R. Abd Rashid, et al., FeCl<sub>3</sub>-activated carbon developed from coconut leaves: characterization and application for methylene blue removal, *Sains Malays.* 47 (3) (2018) 603–610.
- [41] M. Emirie, Removal of Chromium Hexavalent (Cr (VI) from Aqueous Solution Using Activated Carbon Prepared from Prosopis Juliflora Plant and Find the Optimal Operating Condition for Adsorption Process, Addis Ababa University Addis Ababa, 2015.
- [42] T. Adane, et al., Response surface methodology as a statistical tool for optimization of removal of chromium (VI) from aqueous solution by Teff (*Eragrostis teff*) husk activated carbon, *Appl. Water Sci.* 10 (2020) 1–13.
- [43] Q. Cao, et al., Process effects on activated carbon with large specific surface area from corn cob, *Bioresour. Technol.* 97 (1) (2006) 110–115, <https://doi.org/10.1016/j.biortech.2005.02.026>.
- [44] M. Danish, T. Ahmad, A review on utilization of wood biomass as a sustainable precursor for activated carbon production and application, *Renew. Sust. Energ.* 87 (2018) 1–21.
- [45] Y.-b. Tang, Q. Liu, F.-y. Chen, Preparation and characterization of activated carbon from waste ramulus mori, *J. Chem. Eng.* 203 (2012) 19–24, <https://doi.org/10.1016/j.cej.2012.07.007>.
- [46] A. Kumar, H.M. Jena, Preparation and characterization of high surface area activated carbon from Fox nut (*Euryale ferox*) shell by chemical activation with H<sub>3</sub>PO<sub>4</sub>, *Results Phys.* 6 (2016) 651–658.
- [47] G. Issabayeva, M.K. Aroua, N.M.N. Sulaiman, Removal of lead from aqueous solutions on palm shell activated carbon, *Bioresour. Technol.* 97 (18) (2006) 2350–2355, <https://doi.org/10.1016/j.biortech.2005.10.023>.
- [48] J. Bayuo, K.B. Pelig-Ba, M.A. Abukari, Optimization of adsorption parameters for effective removal of lead (II) from aqueous solution, *Indian J. Chem.* 14 (2019) 1–25.
- [49] K. Singh, M. Talat, S. Hasan, Removal of lead from aqueous solutions by agricultural waste maize bran, *Bioresour. Technol.* 97 (16) (2006) 2124–2130, <https://doi.org/10.1016/j.biortech.2005.09.016>.
- [50] D. Adie, et al., Removal of lead ions from aqueous solutions using powdered corn cobs, *Can. J. Chem. Eng.* 88 (2) (2010) 241–255, <https://doi.org/10.1002/cjce.20264>.
- [51] S. Berhe, et al., Adsorption efficiency of coffee husk for removal of lead (II) from industrial effluents: equilibrium and kinetic study, *Int. J. Sci. Res.* 5 (9) (2015) 1–8.
- [52] A. El-Wakil, W. Abou El-Maaty, F. Awad, Removal of lead from aqueous solution on activated carbon and modified activated carbon prepared from dried water hyacinth plant, *J. Anal. Bioanal. Tech.* 5 (2) (2014) 1–14, <https://doi.org/10.4172/2155-9872.1000187>.
- [53] B. Sivakumar, C. Kannan, S. Karthikeyan, Preparation and characterization of activated carbon prepared from balsamodendron caudatum wood waste through various activation processes, *Rasayan J. Chem.* 5 (3) (2012) 321–327.
- [54] S. Charola, et al., Fixed-bed adsorption of reactive Orange 84 dye onto activated carbon prepared from empty cotton flower agro-waste, *Sustain. Environ. Res.* 28 (6) (2018) 298–308, <https://doi.org/10.1016/j.serj.2018.09.003>.
- [55] T.S. Tessema, A.T. Adugna, M. Kamaraj, Removal of Pb (II) from synthetic solution and paint industry wastewater using activated carbon derived from african arrowroot (*Canna indica*) stem, *Adv. Mater. Sci. Eng.* (2020) 2020, <https://doi.org/10.1155/2020/8857451>.
- [56] M.A. Khan, et al., Removal of lead ion from aqueous solution by bamboo activated carbon, *Int. J. Water* 5 (4) (2015) 33–46.
- [57] A. Ladavos, et al., The BET equation, the inflection points of N<sub>2</sub> adsorption isotherms and the estimation of specific surface area of porous solids, *Microporous Mesoporous Mater.* 151 (2012) 126–133.
- [58] D. Xin-Hui, et al., Preparation of activated carbon from Jatropha hull with microwave heating: optimization using response surface methodology, *Fuel Process. Technol.* 92 (3) (2011) 394–400.
- [59] K. Reddy, A. Al Shoaibi, C. Srinivasakannan, Activated carbon from date palm seed: process optimization using response surface methodology, *Waste Biomass Valorization* 3 (2) (2012) 149–156.
- [60] Y. Liu, et al., Material basis research for Huangqi Jianzhong Tang against chronic atrophic gastritis rats through integration of urinary metabonomics and SystemsDock, *J. Ethnopharmacol.* 223 (2018) 1–9.
- [61] A. Murray, B. Örmeci, Competitive effects of humic acid and wastewater on adsorption of Methylene Blue dye by activated carbon and non-imprinted polymers, *J. Environ. Sci.* 66 (2018) 310–317.